Supramolecular Chemistry

Formation of [60]Fullerene Nanoclusters with Controlled Size and Morphology through the Aid of Supramolecular Rod–Coil Diblock Copolymers**

*Norifumi Fujita, Taketomo Yamashita, Masayoshi Asai, and Seiji Shinkai**

It is known that block copolymers can self-organize into a large number of phase-separated superlattices with characteristic dimensions that range from a few nanometers up to several micrometers.[1] The interplay of supramolecular physics and chemistry has opened up several new approaches to the production of inorganic, organic, and biological superstructures and to their integration into functional units.[2] Amphiphilic compounds are frequently utilized as functional matrices in the preparation of these superstructures.[3] In the study of their applications, the importance of controlling the size of nanoparticles has been described; such control was successful particularly in the field of inorganic materials such as metal colloids, quantum dots, and cluster catalysts.[1,4] Examples of controlling the size of their organic counterparts, however, are very limited so far,[5] in spite of their wide range of applications in materials science.

When a solution of diblock copolymer PS(21 400)-*b*-P4VP(20 700) (**A**; PS = polystyrene, *b* = *block*, P4VP = poly(4-vinylpyridine)) is cast on a surface under appropriate conditions, a periodic lamellar structure about 20 nm in diameter is formed as a result of the amphiphilic nature of the copolymer.[6] The very different surface basicities of the PS and P4VP domains allows acidic species only to be selectively assembled on the P4VP domain. For example, when the sol–gel reaction of tetraethoxysilane is carried out on this surface silica grows to form a string structure on the P4VP domain.[6] Herein, we report a supramolecular approach using rod–coil diblock copolymers prepared from random-coil PS-*b*-P4VPs as hosts and [60]fullerene carboxylic acid as a guest that leads to the formation of spherical [60]fullerene nanoclusters with controlled size and morphology, which are changeable depending on the composition of the PS-*b*-P4VPs.[7] The examples described herein would offer one of the most convenient practical methodologies (just by mixing) for the control and fabrication of [60]fullerene nanoparticles.

[*] Dr. N. Fujita, T. Yamashita, M. Asai, Prof. Dr. S. Shinkai
Department of Chemistry & Biochemistry
Graduate School of Engineering, Kyushu University
6-10-1 Hakozaki, Higashi-ku, Fukuoka 812-8581 (Japan)
Fax: (+81) 92-642-3611
E-mail: seijitcm@mbox.nc.kyushu-u.ac.jp

[**] Support was provided by the 21st Century COE Project, Functional Innovation of Molecular Informatics. We would like to thank H. Matsukizono and M. Fujita of Kyushu University for the DLS analysis and AFM measurements, respectively.

Supporting information for this article is available on the WWW under http://www.angewandte.org or from the author.

 DOI: 10.1002/ange.200461174

Polymer **A** (1.0 mg) and [60]fullerene carboxylic acid (**1**, 1.0 mg) were dissolved in 3-pentanone (1.0 mL), and sonicated for one minute at room temperature. The solution

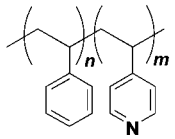

PS-*b*-P4VP

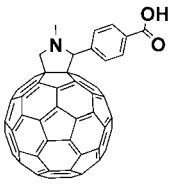

1

became homogeneous and brown in color, thus indicating that **1** had interacted with polymer **A** (since **1** was only partially soluble in 3-pentanone without **A**). A carbon-coated copper grid was immersed in this solution for a few seconds and then dried under ambient conditions for 6 hours. After the sample had been dried in vacuo for 12 hours, it was analyzed by transmission electron microscopy (TEM) without staining.

TEM analysis revealed that the size and morphology of the generated spherical [60]fullerene clusters are quite uniform. Black spheres with a small distribution range of diameters (20–30 nm) are clearly recognized (Figure 1). The

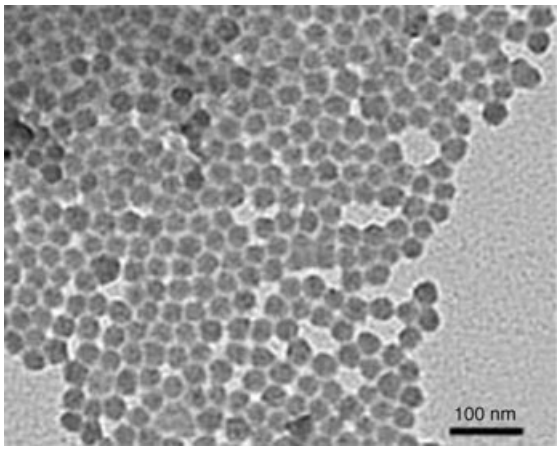

Figure 1. TEM image of polymer **A**·**1** composite.

samples observed by TEM were not stained, and therefore the black contrast is a result of electron absorption by the [60]fullerenes. Thus, one can propose that a carboxylic acid group in **1** interacts with a pyridine moiety in the P4VP block in polymer **A**, which adopts a rodlike rigid conformation because of the structural bulkiness of bound **1** (Figure 2). Thus, the random-coil structure of the P4VP block is transformed into a rodlike rigid structure and accompanied by a decrease in the solubility. The poor solubility of the [60]fullerene-complexed P4VP block and the high solubility of the PS block in 3-pentanone should result in the formation of the micelle-like superstructures seen in Figure 1. To further support this rationale we carried out TEM analysis of five reference samples prepared under similar conditions to those described above: **1** only, PS homopolymer with **1**, P4VP

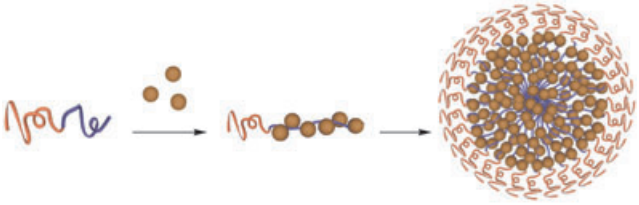

Figure 2. Schematic representation of the formation of supramolecular rod–coil polymers leading to the generation of micelles.

homopolymer with **1**, a mixture of PS and P4VP with **1**, and polymer **A** with unmodified [60]fullerene or with the methyl ester analogue of **1** (**2**, see the Supporting Information). None of these samples shows any spherical or periodic surface structure in the TEM images. Thus, the block composition in the macromolecule and the pyridine–carboxylic acid interaction are indispensable to the formation of such a unique spherical structure.

Spectral analysis of P4VP in the **A**·**1** composite gives an insight into the type of host–guest interactions occurring in this system. The 3-pentanone solvent was removed from the polymer **A**·**1** composite by evaporation, and the resultant brown solid was dried in vacuo and subjected to attenuated total reflectance (ATR) FTIR spectroscopic measurements. The ATR-FTIR spectra of the samples show the formation of the hydrogen bond between the pyridyl group in PS-*b*-P4VP and the carboxylic acid group in **1** very clearly. The **A**·**1** composites were prepared in different molar ratios of **1** (from 0.20 to 1.0 molar equivalents, where the molar equivalent is defined as the molar ratio of the carboxylic acid function in **1** with respect to the pyridyl function in polymer **A**). In the IR spectra (see the Supporting Information), a band at 1597 cm^{-1}, which is assigned to the ring-stretching vibration, is gradually shifted to 1609 cm^{-1}, which is assigned to the hydrogen-bonded pyridyl group.[8] This shift induced by the interaction with the carboxylic acid group becomes larger as the molar ratio of added **1** increases. Samples containing more than 0.6 molar equivalents of **1** result in turbid solutions, which implies that all the pyridyl groups in polymer **A** cannot interact with **1**: at most, 0.6 molar equivalents of **1** can form a hydrogen bond with the pyridyl group in polymer **A**, probably as a result of steric crowding. Analysis of the C=O band in the same IR spectra clearly shows that hydrogen bonding between the pyridyl group in the block copolymer and **1** plays a key role in the formation of nanoparticles[7a] (for details see the Supporting Information). The five samples prepared for the IR experiments were directly subjected to TEM analysis, and all the samples showed a spherical structure similar to that of the TEM image shown in Figure 1.

It is expected that the length of the homopolymer segments in PS-*b*-P4VPs would affect the size and morphology of the [60]fullerene clusters in the core of the micelle-like PS-*b*-P4VP·**1** composites. We thus tried to construct [60]fullerene superstructures with PS-*b*-P4VPs having block segments of different lengths. The [60]fullerene clusters were prepared according to the same conditions as above, where the molar ratio of **1** versus the pyridyl function in the P4VP segment is fixed to 0.6 molar equivalents. Table 1 summarizes

Table 1: Compositions of PS-*b*-P4VPs used and structural parameters of their composites with **1**.

PS-*b*-P4VP	M_n of PS and P4VP [g mol^{-1}]	M_w/M_n of PS-*b*-P4VP	*m*(P4VP)/*n*(PS)	Morphology and size observed by TEM
polymer **A**	21 400/20 700	1.13	0.96	sphere, $d = 20$–30 nm
polymer **B**	31 900/13 200	1.08	0.41	sphere, $d = 20$–25 nm
polymer **C**	35 500/3680	1.06	0.10	sphere, $d = 15$–20 nm
polymer **D**	19 900/29 400	1.15	1.5	sphere and cylinder, $d = 40$ nm, $l = 200$–300 nm
polymer **E**	3300/18 700	1.14	5.6	–
polymer **F**	109 000/27 000	1.15	0.25	sphere, $d = 50$–60 nm

the structures of the PS-*b*-P4VPs used and the resultant size and morphology of the PS-*b*-P4VP·**1** composites observed by TEM. It is seen from Table 1 and Figure 3 that polymers **A**–**C**, which have a shorter P4VP segment length with respect to the PS segment length, tend to form spherical aggregates in which the diameter decreases from 20–30 to 20–25 to 15–20 nm, respectively, as length of the P4VP segment decreases from a P4VP/PS ratio of 0.96:1 to 0.41:1 to 0.10:1, respectively. The superstructure formed when the P4VP/PS ratio in the PS-*b*-P4VPs becomes larger changes to a mixture of sphere and cylinder, as seen in the case of polymer **D** (P4VP/PS = 1.5:1). Furthermore, polymer **E** with a P4VP/PS ratio of 5.6:1 does not form any superstructure, as observed by TEM (not shown). Polymer **F** with a P4VP/PS molar ratio of 0.25:1 also shows spherical morphology when it interacts with **1**.

The specific difference in the superstructure formed can be explained as follows. The [60]fullerenes tend to aggregate into a spherical structure that seems to be a priori the most stable (polymers **A**–**C**, and **F**) when the PS segment has sufficient length to induce solubility to the spherical [60]fullerene clusters. However, the PS domain cannot impart sufficient solubility to the spherical [60]fullerene clusters when the length of the PS segment is relatively short (polymer **D**), and the structure is transformed into a cylindrical morphology. This change results in a decrease in the surface area covered with the PS segment. In the case of polymer **E**, the PS segment is so short that the superstructure requiring coverage by the solvophilic PS segment is no longer created. It is clear, therefore, that the structural morphologies of the composites are sharply correlated with the balance of the solubility of the [60]fullerene clusters and the length of the PS segments.

Dynamic light scattering (DLS) analysis provides information on the diameter of the nanoparticles in solution. Figure 4 shows the size distribution of PS-*b*-P4VP·**1** composites in 3-pentanone solution, and indicates that the diameters of the composites are very narrowly distributed. The diameters of the spherical PS-*b*-P4VP·**1** composites prepared from poly-

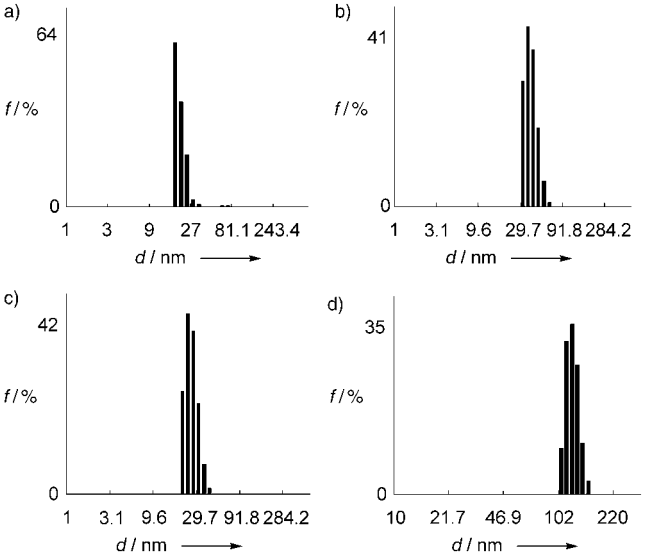

Figure 4. DLS profiles of a) polymer **A**·**1**, b) polymer **B**·**1**, c) polymer **C**·**1**, and d) polymer **F**·**1** composites.

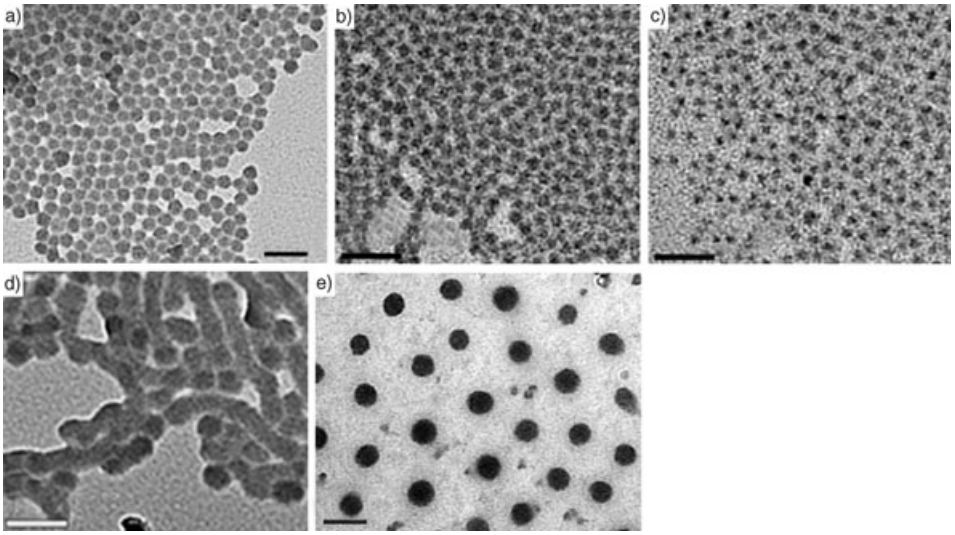

Figure 3. TEM images of PS-*b*-P4VP·**1** composites. a) Polymer **A**·**1**, b) polymer **B**·**1**, c) polymer **C**·**1**, d) polymer **D**·**1**, and e) polymer **F**·**1**. The scale bars correspond to 100 nm.

mers **B**, **C**, and **F** are larger than those determined by TEM. However, the diameter of the spherical PS-*b*-P4VP·**1** composites prepared from polymer **A** is almost the same as that determined by TEM. These discrepancies are rationalized as follows. In the PS-*b*-P4VP·**1** composites obtained from polymers **B**, **C**, and **F**, the molecular weights of the PS segments are sufficiently higher than those of the P4VP segments that the PS corona surrounding the [60]fullerene cluster can be extended into the bulk solution. This situation results in the diameters determined by DLS studies being larger than those determined by TEM. In the case of polymer **A**, however, the molecular weight of the PS segment is comparable to that of the P4VP segment and the PS corona is mainly distributed near the surface of the [60]fullerene cluster. As a result, the diameter of the **A**·**1** composite determined by DLS studies is nearly the same as that determined by TEM.

The size and morphology of the composites can be directly confirmed by scanning electron microscopy (SEM, Figure 5a), which supports the narrow size distribution of the polymer **A**·**1** composite. The diameter of the spherical nanoparticles seen in Figure 5a is comparable with that observed by DLS measurements. Furthermore, the AFM image of the **A**·**1** composite in Figure 5b also shows the spherical morphology with a diameter of about 20 nm. These results consistently support the view that the [60]fullerene clusters created from the PS-*b*-P4VP·**1** composites are stable both in solution and on the surface, even under ultrahigh vacuum conditions.

Mixing two different PS-*b*-P4VP copolymers with **1** provided a very interesting result. Firstly, it was confirmed from TEM analysis that when polymer **A** or **F**, which have long PS block segments, is mixed with **1** in 3-pentanone, the resultant composites show small or large black dots with diameters of 20–30 or 50–60 nm, respectively. Next, polymer **A** (1.0 mg), polymer **F** (1.0 mg), and **1** (2.4 mg) were dissolved together in 3-pentanone (2.0 mL). Interestingly, the TEM image of the sample prepared from this solution shows two different small and large black dots, with the smaller dots excluded from the peripheral area of the larger dots; thus, this finding clearly shows the presence of the PS corona region (Figure 6a). These observations imply that the two copolymers tend to aggregate with **1** separately, thus inducing an intriguing phase-separation phenomenon in the same solution. It is energetically unfavorable for polymers **A** and **F**, which have different block compositions, to form a mixed aggregate in the 3-pentanone solution, because their rod–coil shapes are mismatched (Figure 6b). As a result, the formation of two "homo" aggregates is more stable than that of one "mixed" aggregate.

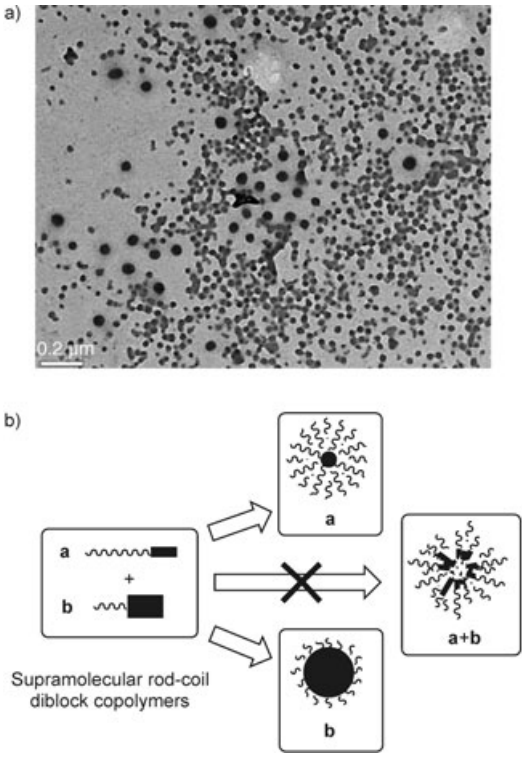

Figure 6. a) TEM image of the sample prepared from a mixture of **1** and polymers **A** and **F** in 3-pentanone. b) Schematic representation of "homo" aggregation processes.

In summary, we have demonstrated the construction of novel supramolecular aggregates by utilizing the formation of hydrogen bonds between host block copolymers and a guest [60]fullerene carboxylic acid. Treatment of these supramolecular rod–coil diblock copolymers under appropriate conditions led to the creation of [60]fullerene nanoparticles with narrow distributions in size and morphology. This methodology is also applicable to the controlled construction of other organic nanoparticles. It is well-known that control of the size and morphology of nanoparticles plays an important role in nanomaterials chemistry; therefore, the methodology de-

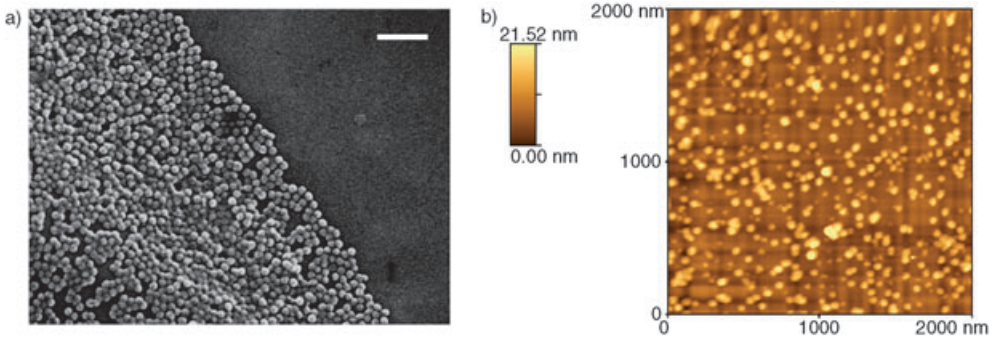

Figure 5. a) SEM and b) AFM images of polymer **A**·**1** composite. The scale bar in the SEM image corresponds to 200 nm and the side of the AFM image is 2 μm long.

scribed here should provide a novel approach to nanomaterials chemistry and functions. The organic nanoparticles obtained from these experiments should show interesting redox, electrochemical, and photochemical properties.

Experimental Section

The block copolymers and [60]fullerene carboxylic acid (**1**) were dissolved in 3-pentanone in a capped test tube and the mixture was sonicated (IUCHI, VS-150) in a water bath at room temperature at a power level of 150 W (50 kHz). The solution became homogeneous after 1 min. This sonication procedure did not affect the polymers or **1**, as confirmed by gel-permeation chromatography and mass spectrometry. A carbon-coated copper grid was immersed in the solution and dried under ambient conditions for 6 h. After drying the sample in vacuo for 12 h at room temperature, it was subjected to TEM observation.

Received: July 3, 2004
Revised: November 12, 2004
Published online: January 20, 2005

Keywords: block copolymers · fullerenes · host–guest systems · nanostructures · supramolecular chemistry

[1] For recent reviews, see: a) S. Förster, T. Plantenberg, *Angew. Chem.* **2002**, *114*, 712 – 739; *Angew. Chem. Int. Ed.* **2002**, *41*, 688 – 714; b) S. Förster, M. Antonietti, *Adv. Mater.* **1998**, *10*, 195 – 217.

[2] For recent work, see: D. M. Vriezema, J. Hoogboom, K. Velonia, K. Takazawa, P. C. M. Cristianen, J. C. Maan, A. E. Rowan, R. J. M. Nolte, *Angew. Chem.* **2003**, *115*, 796 – 800; *Angew. Chem. Int. Ed.* **2003**, *42*, 772 – 776, and references therein; for recent reviews, see: I. W. Hamley, *Angew. Chem.* **2003**, *115*, 1730 – 1752; *Angew. Chem. Int. Ed.* **2003**, *42*, 1692 – 1712.

[3] For selected papers, see: a) Y. N. C. Chan, R. R. Schrock, R. E. Cohen, *Chem. Mater.* **1992**, *4*, 24 – 27; b) J. P. Spatz, S. Mößmer, M. Möller, *Chem. Eur. J.* **1996**, *2*, 1552 – 1555; c) M. Antonietti, S. Förster, J. Hartmann, S. Oestreich, *Macromolecules* **1996**, *29*, 3800 – 3806; d) S. Klingelhöfer, W. Heitz, A. Greiner, S. Oestreich, S. Förster, M. Antonietti, *J. Am. Chem. Soc.* **1997**, *119*, 10116 – 10120; e) M. Moffitt, L. McMahon, V. Pessel, A. Eisenberg, *Chem. Mater.* **1995**, *7*, 1185 – 1192; f) M. Möller, J. P. Spatz, *Curr. Opin. Colloid Interface Sci.* **1997**, *2*, 177 – 187; g) V. Sankaran, J. Yue, R. E. Cohen, R. R. Schrock, *J. Am. Chem. Soc.* **1993**, *115*, 4409 – 4410; h) O. A. Platonova, L. M. Bronstein, S. P. Solodovnikov, I. M. Yanovskaya, E. S. Obolonkova, P. M. Valetsky, E. Wenz, M. Antonietti, *Colloid Polym. Sci.* **1997**, *275*, 426 – 431; i) A. V. Kabanov, S. V. Vinogradov, Y. G. Suzdaltseva, V. Y. Alakhov, *Bioconjugate Chem.* **1995**, *6*, 639 – 643.

[4] R. Schlögl, S. Bee, A. Hamid, *Angew. Chem.* **2004**, *116*, 1656 – 1667; *Angew. Chem. Int. Ed.* **2004**, *43*, 1628 – 1637, and references therein.

[5] H. Kasai, S. Okazaki, T. Hanada, S. Okada, H. Oikawa, T. Adschiri, K. Arai, K. Yase, H. Nakanishi, *Chem. Lett.* **2000**, 1392 – 1393, and references therein.

[6] N. Fujita, H. Otsuka, A. Takahara, S. Shinkai, *Chem. Lett.* **2003**, *32*, 352 – 353.

[7] For representative examples of self-assemblies of polymeric supramolecules, see: a) T. Kato, J. M. J. Fréchet, *Macromolecules* **1989**, *22*, 3818 – 3819; b) O. Ikkala, G. ten Brinke, *Science* **2002**, *295*, 2407 – 2409, and references therein.

[8] a) A. Sidorenko, I. Tokarev, S. Minko, M. Stamm, *J. Am. Chem. Soc.* **2003**, *125*, 12211 – 12216; b) H. Peng, D. Chen, M. Jian, *Langmuir* **2003**, *19*, 10989 – 10992.

